

# Decoherence and quantum contextuality

A. S. Sanz<sup>1</sup> and F. Borondo<sup>2</sup>

<sup>1</sup> Instituto de Física Fundamental, Consejo Superior de Investigaciones Científicas, Serrano 123, 28006 Madrid, Spain  
e-mail: [asanz@imaff.cfmac.csic.es](mailto:asanz@imaff.cfmac.csic.es)

<sup>2</sup> Instituto Mixto de Ciencias Matemáticas CSIC–UAM–UC3M–UCM, and Departamento de Química, C–IX, Universidad Autónoma de Madrid, Cantoblanco – 28049 Madrid, Spain  
e-mail: [f.borondo@uam.es](mailto:f.borondo@uam.es)

Received: February 6, 2020/ Revised version: February 6, 2020

**Abstract.** Decoherence is the most widely accepted mechanism to explain the loss of coherence in quantum systems. Here we show how simple (quantum) trajectory–based models can help to understand the physics behind decoherence processes. In particular, we will analyze with these models the relationship between decoherence and quantum contextuality in the double–slit experiment, where two (quantum) contexts can be clearly distinguished: (i) two slits open simultaneously, or (ii) only one slit open at a time.

**PACS.** 03.65.-w Quantum mechanics (general) – 03.65.Ta Foundations of quantum mechanics; measurement theory – 03.65.Yz Decoherence; open systems; quantum statistical methods – 03.75.Dg Atom and neutron interferometry

## 1 Introduction

Decoherence is the most widespread mechanism [1,2,3,4] to explain the classical–like behavior displayed by quantum systems under certain conditions [5]. According to it, this behavior results from the dynamical interaction between the system of interest and a surrounding environment [6]. If system plus environment are initially described by a separable total wave function, their coupling will make this wave function to describe an *entangled* state after some time. This leads to dramatic consequences for the system, which is no longer describable in terms of its own wave function, but a density matrix. Thus, if we start it within a *pure state*, after averaging over the environment degrees of freedom at any subsequent time, one gets a *mixed state*. The entanglement with an environment provokes the loss of coherence in the system —coherence which is necessary to keep the system in a pure state and display typical quantum effects, such as diffraction–like structures, for instance. This irreversible process is an important issue, not only for practical purposes, for instance, in modern quantum information theory or quantum computation [7], but also in more fundamental aspects of quantum mechanics, as will be discussed below.

Quantum mechanics is characterized by different striking features or properties which puzzle and challenge our understanding, *contextuality* being one of the most remarkable and fundamental ones. Quantum contextuality implies that the physics associated with a certain system unavoidably depends on the quantum state chosen to de-

scribe it. In other words, unlike classical systems for which only external forces determine their dynamics, the behavior of quantum–mechanical systems is also governed by the contextual framework chosen to carry out their description. The information about this contextual framework is coded within the wave function, which accounts for the system quantum state (and its subsequent evolution). This aspect of quantum mechanics, which has no classical analog, nicely manifests in and explains the paradigmatic double–slit experiment [8].

Far from being a conceptual idealization, diffraction by slits is a realizable experiment, which has been done with a variety of projectiles ranging from tinny electrons [9] to large, complex fullerenes [10]. These experiments are generally carried out by sending a particle beam towards the slits (i.e., many particles at a time targeted towards the slit assembly). However, they can also be performed launching the projectiles one by one (i.e., one at a time). Let us consider the case where the target is just a double–slit. As is well–known, provided no “which–way” information is demanded, the diffracted projectiles distribute according to a typical diffraction pattern, which is described by the probability density

$$\begin{aligned} \rho(\mathbf{r}, t) &= |\psi_1(\mathbf{r}, t) + \psi_2(\mathbf{r}, t)|^2 \\ &= \rho_1(\mathbf{r}, t) + \rho_2(\mathbf{r}, t) + \rho_{\text{int}}(\mathbf{r}, t). \end{aligned} \quad (1)$$

Here  $\psi_i(\mathbf{r}, t)$  ( $i = 1, 2$ ) is the (time–dependent) wave function describing the particle after passing through slit  $i$  and  $\rho_i(\mathbf{r}, t) = |\psi_i(\mathbf{r}, t)|^2$  is the probability that such a particle is detected at the position  $\mathbf{r}$  at a time  $t$  after passing *only*

through this slit. Regardless of the nature of the particle source [11,12], particles are assumed as *independent* after they abandon it, this being the meaning of “one by one” above. Equation (1) thus describes a *single-particle* experiment rather than a many-body situation. This is a key point: the “standard” explanation of this experiment [8] states that the interference-like features [accounted for by  $\rho_{\text{int}}$  in equation (1)] are due to the interference of the particle with itself (*self-interference*). That is, when reaching the two slits, the particle passes through *both* at the same time, and then “recombines” again behind, thus giving rise to the well-known quantum interference pattern. On the contrary, if a detector aimed to determine the path followed by the particle is allocated in one of the slits, a classical like probability distribution is obtained,

$$\begin{aligned} \rho(\mathbf{r}, t) &= |\psi_1(\mathbf{r}, t)|^2 + |\psi_2(\mathbf{r}, t)|^2 \\ &= \rho_1(\mathbf{r}, t) + \rho_2(\mathbf{r}, t). \end{aligned} \quad (2)$$

Obviously, since there is only one possible path, self-interference disappears and no interference pattern is observed.

The two outcomes mentioned above are commonly related in standard quantum mechanics textbooks [13] to the well-known wave-corpucle duality. If quantum particles behave like waves (and therefore undergo self-interference), interference patterns are observed; if they behave as corpuscles, their distribution follows a classical-like addition rule for probabilities [as expressed in equation (2)]. On the other hand, this behavior can also be related to the measurement problem [14]: since two canonically conjugate variables in quantum mechanics cannot be simultaneously determined, measuring one of them with infinite precision will avoid doing the same with the other one [13]. In a double-slit experiment, if we want to know which slit is traversed by the particle, the interference pattern will not be observed because self-interference information is “destroyed”. Conversely, the particle momentum can be measured by letting the particle reaching the detector, which also yields the formation of the interference pattern. However, no clue on the way followed by the particle (“which-way” information) is then obtained.

The two outcomes in a two-slit experiment can also be understood in the light of a third alternative viewpoint: quantum contextuality. Accordingly, these outcomes are regarded as two totally different experimental contexts. One of them, say experiment *A*, is arranged in such a way that both slits are considered open at the same time. In the other one, *B*, only one slit is open. Thus, within this framework (and putting aside any external action), particle dynamics is ruled by the information of how many slits are open. Note that the previous viewpoints (duality and position-momentum measurements) are in accordance with considering that either we have one experiment or the other. More importantly, this viewpoint is objective: it is the experiment itself, not an external observer, what determines the final outcome observed. In other words, once the “rules of the game” are established, namely, the initial state of the system,  $\Psi_0$ , and the external potential,  $V(\mathbf{r})$ , describing the initial context and the subsequent

evolution of the system, there are no paradoxes (subjectivity).

After the context is defined, any eventual action of an external observer should be considered as a change of such a context and therefore the initial description will no longer be valid. One can find situations where a partial suppression of the interference is observed in the intensity pattern measured [15,16]. Assuming that this suppression is gradual, this effect can be thought as a smooth transition from the context defined by experiment *A* to the other one, defined by experiment *B*. For this process to happen, one has then to invoke decoherence as the mechanism leading to such a transition process. Let us assume, for instance, that the environment consists of many randomly distributed particles interacting with the system by means of scattering processes. When these events occur in a large number, the off-diagonal elements of the system reduced density matrix undergo an exponential damping [17] (within a Markovian regime), and the system loses quickly its coherence.

In this paper we illustrate the problem of quantum contextuality and decoherence within a simple quantum-trajectory scenario [18,19,20]. The reason to use such an approach (instead of wave functions or density matrices) is because trajectories allow us to follow the system dynamics and to understand the underlying physics at the same level that classical trajectories help to understand the classical world. In this sense, quantum trajectories have clear interpretational and pedagogical advantages. To make the paper self-contained, we will first briefly review in Section 2 decoherence in two-slit interference problems from the standard quantum mechanical point of view. In Section 3 we introduce the trajectory formulation of quantum mechanics, also known as *Bohmian mechanics*, as well as the problems involved when dealing with many degrees of freedom and how they can be “skipped” by the use of the so-called *reduced trajectories* [21]. In Section 4 we illustrate the ideas described in the previous sections by using the experimental data of the two-slit experiment with cold neutrons carried out by Zeilinger *et al.* [22]. Finally, in Section 5 we summarize the main conclusions derived from this work.

## 2 Decoherence in the double-slit experiment

Rigorous studies on quantum decoherence are usually carried out by means of relatively complicated theoretical formalisms. When the environment dynamics is irrelevant and the model can be considered as Markovian, different approaches based on solving either master equations for the reduced density matrix [23,24] or stochastic wave equations [25] can be used. Otherwise, more complicated trajectory based techniques [24,26] (e.g., semiclassical initial value representation [27]) are usually considered in order to account for the environment dynamics and its effects on the system of interest. Nevertheless, sometimes it is possible to devise simple models which allow us to understand how the coherence damping takes place, in particular, in double-slit experiments [28,29,30], which we

are interesting in here. For instance, provided dephasing effects (energy relaxation) are negligible during the system time-evolution, the double-slit experiment with decoherence can be described by means of simple phenomenological models, as done in reference [31]. Next, we will describe the main features of this model; a more thorough discussion of it can be found in reference [31].

Consider a particle after passing through a double-slit assembly. In the absence of interactions with an environment, the time-evolution [32] for this particle is described by the wave function

$$|\Psi^{(0)}\rangle_t = c_1|\psi_1\rangle_t + c_2|\psi_2\rangle_t, \quad (3)$$

where  $|\psi_j\rangle_t$  is the *partial* wave emerging from the slit  $j$  (with  $j = 1, 2$ ) and  $|c_1|^2 + |c_2|^2 = 1$  at any time. In the coordinate representation, the associate density matrix,  $\hat{\rho}_t^{(0)} \equiv |\Psi^{(0)}\rangle_t \langle\Psi^{(0)}|$ , reads as

$$\rho_t^{(0)}(\mathbf{r}, \mathbf{r}') = \Psi_t^{(0)}(\mathbf{r}) \left[ \Psi_t^{(0)}(\mathbf{r}') \right]^*, \quad (4)$$

with  $\Psi_t^{(0)}(\mathbf{r}) = \langle \mathbf{r} | \Psi^{(0)} \rangle_t$ . The diagonal of equation (4) gives the probability density (measured intensity),

$$\rho_t^{(0)}(\mathbf{r}) = |c_1|^2 |\psi_1|_t^2 + |c_2|^2 |\psi_2|_t^2 + 2|c_1||c_2||\psi_1|_t|\psi_2|_t \cos \delta_t, \quad (5)$$

with  $\delta_t$  being a space and time dependent phase-shift between the two partial waves.

Under the presence of an environment, (3) is no longer valid to describe the (reduced) system dynamics. In this case, first the total system (i.e., system of interest plus environment) is initially represented as

$$|\Psi\rangle = |\Psi^{(0)}\rangle \otimes |E_0\rangle \quad (6)$$

at  $t = 0$ , with  $|\Psi^{(0)}\rangle$  as in equation (3). Then, assuming that the environment acts differently on each diffracted beam [28,31], at time  $t$  we will have

$$|\Psi\rangle_t = c_1|\psi_1\rangle_t \otimes |E_1\rangle_t + c_2|\psi_2\rangle_t \otimes |E_2\rangle_t. \quad (7)$$

That is, the coupling between the environment and the system makes the environment states (which start from  $|E_1\rangle = |E_2\rangle = |E_0\rangle$  at  $t = 0$ ) evolving to  $|E_1\rangle_t \neq |E_2\rangle_t$  at a time  $t$ . The total wave function thus becomes an *entangled state*. The reduced probability density associated with the system of interest is now obtained from (7) by tracing the full density matrix,  $\hat{\rho}_t \equiv |\Psi\rangle_t \langle\Psi|$ , over the environment states. This leads to

$$\hat{\rho}_t = \sum_{j=1}^2 \langle E_j | \hat{\rho}_t | E_j \rangle_t. \quad (8)$$

Note that, in the coordinate representation and for an environment constituted by  $N$  particles, equation (8) should be obtained after integrating  $\tilde{\rho}_t(\mathbf{r}, \mathbf{r}')$  over the  $3N$  environment degrees of freedom, i.e.,

$$\tilde{\rho}_t(\mathbf{r}, \mathbf{r}') = \int \langle \mathbf{r}, \mathbf{r}_1, \mathbf{r}_2, \dots, \mathbf{r}_N | \Psi \rangle_t \times \langle \Psi | \mathbf{r}', \mathbf{r}_1, \mathbf{r}_2, \dots, \mathbf{r}_N \rangle_t d\mathbf{r}_1 d\mathbf{r}_2 \dots d\mathbf{r}_N. \quad (9)$$

with  $\{\mathbf{r}_i\}_{i=1}^N$ ,  $\mathbf{r}_i$  being a 3-dimensional vector. Substituting (7) into equation (8), rearranging terms and expressing the final result in the reduced coordinate representation, one reaches

$$\tilde{\rho}_t(\mathbf{r}, \mathbf{r}') = (1 + |\alpha_t|^2) \sum_{j=1}^2 |c_j|^2 \psi_{j,t}(\mathbf{r}) \psi_{j,t}^*(\mathbf{r}') + 2\alpha_t c_1 c_2^* \psi_{1,t}(\mathbf{r}) \psi_{2,t}^*(\mathbf{r}') + c.c., \quad (10)$$

where  $\alpha_t \equiv \langle E_2 | E_1 \rangle_t$  and *c.c.* means the conjugate complex. From equation (10) the measured intensity results

$$\tilde{\rho}_t = (1 + |\alpha_t|^2) [|c_1|^2 |\psi_1|_t^2 + |c_2|^2 |\psi_2|_t^2 + 2A_t |c_1||c_2||\psi_1|_t|\psi_2|_t \cos \delta'_t], \quad (11)$$

with

$$A_t \equiv \frac{2|\alpha_t|}{(1 + |\alpha_t|^2)} \quad (12)$$

being the *coherence degree* [31], which gives an idea of the *fringe visibility*. In the particular where  $|\alpha_t| = e^{-t/\tau_c}$ ,  $\tau_c$  being the coherence time, one obtains

$$A_t = \text{sech}(t/\tau_c), \quad (13)$$

which establishes a simple relationship between the degree of coherence and the coherence time. Although  $\tau_c$  can be determined by means of detailed theoretical models [29, 30], where  $\tau_c$  is a function of different physical parameters (e.g., the system mass or the temperature), the model here described allows us to have an estimate of its value from the experiment.

As can be clearly seen, asymptotically equation (11) approaches

$$\tilde{\rho}_t = |c_1|^2 |\psi_1|_t^2 + |c_2|^2 |\psi_2|_t^2, \quad (14)$$

which follows the classical addition rule for probabilities when there are two possible outcomes. Moreover, also note that although it has been applied to the double-slit, this model is suitable for the study any interference process affected by decoherence, since equation (14) is valid in general.

After equation (14), a doubt now arises: Is this a classical-like result, or is there still some quantumness within it? In next Section we provide a suitable model to answer this question.

## 3 Quantum trajectory models for decoherence

### 3.1 Bohmian trajectories

The above described double-slit experiment with decoherent can be understood in terms of the so-called *reduced quantum trajectories*, proposed in reference [21]. These trajectories satisfy equations of motion similar to those

arising in Bohmian mechanics [18, 19, 20], but with an important difference: the environment dynamics is not explicitly considered, but only its effects on the system reduced density matrix.

Given a general probability density  $\rho_t(\mathbf{r})$ , its time-evolution is determined by the equation of motion

$$\frac{\partial \rho_t(\mathbf{r})}{\partial t} = -\nabla \cdot \mathbf{J}_t(\mathbf{r}), \quad (15)$$

which can be understood as the continuity equation of a *quantum flow*, where  $\mathbf{J}_t$  is the so-called *probability current density*,

$$\mathbf{J}_t \equiv \frac{\hbar}{2im} [\Psi_t^* \nabla \Psi_t - (\nabla \Psi_t^*) \Psi_t]. \quad (16)$$

The quantum fluid dynamics described by  $\rho_t$  and  $\mathbf{J}_t$  can also be derived from the wave function as follows. We first rewrite it in polar form

$$\Psi_t(\mathbf{r}) = \rho_t^{1/2}(\mathbf{r}) e^{iS_t(\mathbf{r})/\hbar}, \quad (17)$$

where  $\mathbf{J}_t \equiv \rho_t \nabla S_t / m$ , with

$$S_t \equiv \frac{\hbar}{2i} \ln \left( \frac{\Psi_t}{\Psi_t^*} \right). \quad (18)$$

Introducing equation (16) into the time-dependent Schrödinger equation and then separating the real and imaginary parts of the resulting expression, one obtains

$$\frac{\partial S_t}{\partial t} = -\frac{(\nabla S_t)^2}{2m} - V_t^{\text{eff}}, \quad (19)$$

where

$$V_t^{\text{eff}} \equiv V + Q_t = V - \frac{\hbar^2}{2m} \frac{\nabla^2 \rho_t^{1/2}}{\rho_t^{1/2}}, \quad (20)$$

and the continuity equation given by equation (15), respectively. Equation (19) is the *quantum Hamilton–Jacobi equation*, from which the equations of motion for the quantum particles are assumed to be

$$\dot{\mathbf{r}}_t \equiv \frac{\mathbf{J}_t}{\rho_t} = \frac{\hbar}{2im\rho_t} [\Psi_t^* \nabla \Psi_t - (\nabla \Psi_t^*) \Psi_t]. \quad (21)$$

This trajectory-based reformulation of standard quantum mechanics is the so-called Bohmian mechanics. It is based on the calculation of quantum flows or trajectories (particles are always regarded as particles affected by a physical wave field) and is totally equivalent to standard quantum mechanics. In particular, it has been widely used to describe quantum interference and diffraction [34, 35, 36, 37].

### 3.2 Reduced quantum trajectories

As it also happens for the standard version of quantum mechanics, a direct application of Bohmian mechanics to decoherence problems is numerically prohibitive due to the large number of degrees of freedom involved. However, and similarly to standard quantum Markovian models, the difficulties coming from the many-body problem

involved can be avoided by “averaging” the action of the environment degrees of freedom in the Bohmian motion. This is the philosophy of the reduced quantum trajectory formalism proposed in reference [21]. Although these trajectories are still affected by the environment, it is not necessary to consider its dynamics (i.e., to compute the exact multi-dimensional Bohmian trajectories which describe the system-plus-environment dynamics in a “wholistic” way), since the expression of the (system) particle velocity does not depend explicitly on the environment degrees of freedom within this formulation. This is a great advantage: the reduced quantum trajectories provide an important insight into the system dynamics, keeping simultaneously the same features existing in standard Bohmian mechanics (e.g., the momentum single-valuation) at a low computational cost.

In order to account for the action of the environment on the system, it is more appropriate to express  $\mathbf{J}_t$  in terms of the density matrix, i.e.,

$$\mathbf{J}_t \equiv \frac{\hbar}{m} \text{Im}[\nabla_{\mathbf{r}} \rho_t^{(0)}(\mathbf{r}, \mathbf{r}')] \Big|_{\mathbf{r}'=\mathbf{r}}, \quad (22)$$

rather than using equation (9). Under the presence of the environment, equation (22) becomes

$$\tilde{\mathbf{J}}_t \equiv \frac{\hbar}{m} \text{Im}[\nabla_{\mathbf{r}} \tilde{\rho}_t(\mathbf{r}, \mathbf{r}')] \Big|_{\mathbf{r}'=\mathbf{r}}, \quad (23)$$

which satisfies the continuity equation

$$\frac{\partial \tilde{\rho}_t}{\partial t} = -\nabla \tilde{\mathbf{J}}_t. \quad (24)$$

From equations (23) and (24), the velocity field,  $\dot{\tilde{\mathbf{r}}}_t$ , associated with the reduced system dynamics can be defined according to the relation

$$\tilde{\mathbf{J}}_t = \tilde{\rho}_t \dot{\tilde{\mathbf{r}}}_t. \quad (25)$$

This field is the reduced analog of the Bohmian velocity field given by equation (21). The reduced quantum trajectories are now obtained integrating the equation of motion

$$\dot{\tilde{\mathbf{r}}}_t \equiv \frac{\hbar}{m} \frac{\text{Im}[\nabla_{\mathbf{r}} \tilde{\rho}_t(\mathbf{r}, \mathbf{r}')] \Big|_{\mathbf{r}'=\mathbf{r}}}{\text{Re}[\tilde{\rho}_t(\mathbf{r}, \mathbf{r}')] \Big|_{\mathbf{r}'=\mathbf{r}}} \quad (26)$$

(for simplicity, from now on we are not going to use the ‘tilde’ when referring to the reduced trajectory  $\tilde{\mathbf{r}}_t$ ). The dynamics described by this equation leads to the correct intensity pattern when the statistics of a large particle ensemble is considered [21] (see below in Section 4). Moreover, it can be easily shown [21] that equation (26) reduces to the well-known expression for the Bohmian velocity field when there is no interaction with the environment.

### 3.3 Screened trajectories

*A priori* one would expect the quenching produced by the environment [see equations (11) and (12)] in the interference pattern to be equivalent to a gradual loss of information about the slit that the particle does not traverse (for

simplicity, from now on we will denote such a slit as the “empty” slit). That is, the influence of the corresponding “empty” wave on the particle motion should also decrease. However, as inferred from equation (14), the quantum motion will keep information about the initial context (both slits open) even in conditions with total suppression of interference. Note that in the limit of full quenching ( $t \gg \tau_c$ ,  $\alpha_t \rightarrow 0$ ), equation (26) becomes

$$\dot{\mathbf{r}}_t = \frac{|c_1|^2 \rho_t^{(1)} \dot{\mathbf{r}}_1 + |c_2|^2 \rho_t^{(2)} \dot{\mathbf{r}}_2}{\rho_t^{\text{cl}}}, \quad (27)$$

where  $\dot{\mathbf{r}}_j$  and  $\rho_t^{(j)}$  are, respectively, the velocity field and the probability density associated with the partial wave  $|\psi_j\rangle_t$ , and

$$\rho_t^{\text{cl}} \equiv |c_1|^2 \rho_t^{(1)} + |c_2|^2 \rho_t^{(2)}. \quad (28)$$

In this limit, both  $\rho_t^{\text{cl}}$  and the current density,

$$\mathbf{J}_t^{\text{cl}} \equiv \rho_t^{\text{cl}} \dot{\mathbf{r}}_t = |c_1|^2 \rho_t^{(1)} \dot{\mathbf{r}}_1 + |c_2|^2 \rho_t^{(2)} \dot{\mathbf{r}}_2, \quad (29)$$

are, therefore, properly defined. The former is a sum of partial probability densities and the latter a sum of the current densities corresponding to each slit independently considered. Moreover, in both cases probabilities and current densities are properly weighted through the normalizing prefactors  $|c_1|^2$  and  $|c_2|^2$ . Thus, although the particle statistics reproduces the classical-like results, the quantum motion is determined by both slits: although the preferential directions along diffraction channels gradually disappear, trajectories cannot cross the symmetry axis between the slits [36], this being a signature of the empty-slit information. In order to observe a full transition towards a classical-like regime within the theoretical framework here described, an erasure of the empty-slit information is necessary. Any mechanism producing this effect should be similar to consider a gradual *screening* or *dissipation* of the empty-slit information.

As seen in Section 2, from a standard quantum mechanical viewpoint, a two-slit experiment with full decoherence is equivalent to another one performed with each slit independently open. However, when this situation is studied in terms of reduced quantum trajectories something different happens, as seen above. Although the diffraction-like pattern is destroyed, particles still move under the guidance of both partial waves, since decoherence does not account for the erasure of the information about the initial presence of two slits. In order to include this erasing process, it is important to note the following. Within an exact Bohmian framework, the limit discussed above should be such that the corresponding quantum trajectories would behave as if they were not aware of the existence of a double-slit. That is, particles started with initial conditions chosen on one of the two slits should evolve losing gradually the information regarding the other slit. Bohmian trajectories cannot pass through the same point in configuration space at the same time. Thus, the crossings that one would observe in the reduced system space due to the loss of empty-slit information have to be understood as projections of  $3(N+1)$ -dimensional trajectories on this space. Somehow, this situation resembles what

happens in classical mechanics, where trajectories can pass through the same point of the coordinate space at the same time, but not in phase space. The reduced quantum trajectories defined by equation (26) also preserve the single-valuedness property, although it directly emerges in the system subspace since the environment dynamics is not considered explicitly.

Now, in order to reproduce the behavior of the projections of the exact Bohmian trajectories in the system subspace, we can consider the following simple trajectory model, which gathers both decoherence and loss of empty-slit information. In analogy to  $\alpha_t$ , we can also assume that the influence of the empty slit on the particle motion decreases exponentially, due to an increasing entanglement with the environment. At the same time, the loss of information about the empty slits is balanced by a gain of information about the traversed one. Thus, if the particle passes through one of the slits, say 1, the coefficient associated with  $|\psi_2\rangle_t$  is expressed as  $c'_2 = c_2 e^{-t/\tau_s}$ , where  $\tau_s$  is the *screening time*, i.e., a time scale that measures the loss of empty-slit information. This characteristic time is a measure of how fast the information provided by the empty wave is decoupled from the particle motion. On the other hand, the coefficient for  $|\psi_1\rangle_t$  will be

$$c'_1 = c_1 \sqrt{(1 - |c_2|^2 e^{-2t/\tau_s}) / |c_1|^2}, \quad (30)$$

indicating the increasing role of the traversed slit. Taking this into account, the evolution of the system can be described by equation (26), but replacing the coefficients  $c_i$  by their respective time-dependent counterparts,  $c'_i$ .

Since there are two characteristic times,  $\tau_s$  and  $\tau_c$ , a ratio  $\eta \equiv \tau_s/\tau_c$  can be defined from which two different dynamical regimes emerge. If  $\eta \ll 1$ , the particle loses the information about the empty slit (say 2) relatively fast, and equation (26) would then reduce to

$$\dot{\mathbf{r}}_t = \dot{\mathbf{r}}_1, \quad (31)$$

i.e., the motion of the particle is asymptotically only affected by the traversed slit before decoherence takes place. Notice that, statistically, this situation leads to the same kind of pattern obtained directly from equation (27). However, the particle dynamics is totally different: particles are allowed to cross the symmetry axis of the experiment because, at a given time, the momentum can have two different values on the same space point, as in classical mechanics. On the other hand, if  $\eta \gg 1$ , the interference quenching takes place before the motion of the particle becomes fully decoupled and equation (26) remains basically the same during the system evolution. Obviously, this expression will approach equation (31) asymptotically, since the information related to the empty slit will be gradually suppressed.

To conclude this subsection, we would like to stress that what has been presented here is a simple model, in which dissipation plays a very important role, and therefore the continuity equation is not satisfied. However, the model is very helpful in the sense that it provides an understandable and intuitive insight into dynamics going

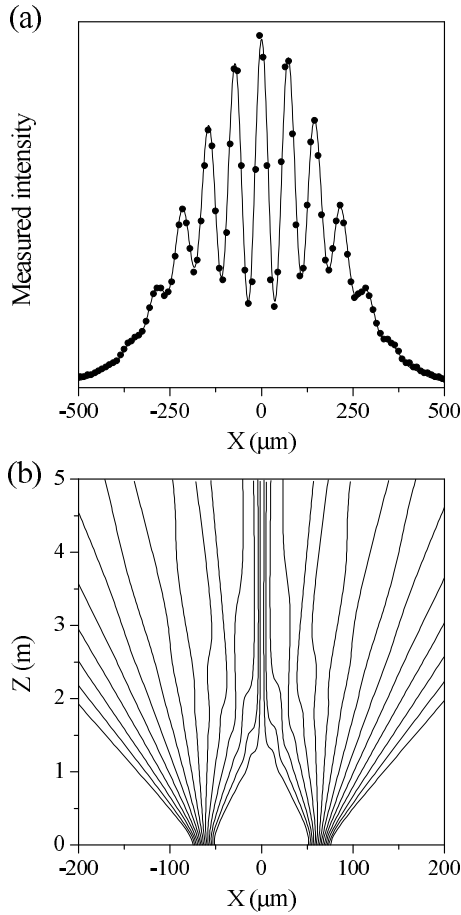


**Fig. 1.** a) Intensity obtained from reduced quantum trajectory (●) and standard quantum mechanics (solid line) calculations for a double-slit experiment with cold neutrons. b) Sample of reduced quantum trajectories illustrating the dynamics associated with the results shown in part (a).

from a linear theory with single-valued momenta to an “apparent” non-linear one, where the momentum can be multi-valued.

## 4 A simple simulation

In this Section we illustrate the ideas discussed above using as a working model the double-slit experiment performed by Zeilinger *et al.* [22] with cold neutrons. This model has been thoroughly analyzed elsewhere [31] from both the optical and the standard quantum mechanical points of view.

### 4.1 Interference quenching

In Figure 1 we present our results for the intensity corresponding to Zeilinger’s experiment obtained with our reduced quantum trajectories method. As can be seen in panel (a), the statistics over trajectories shows an excellent

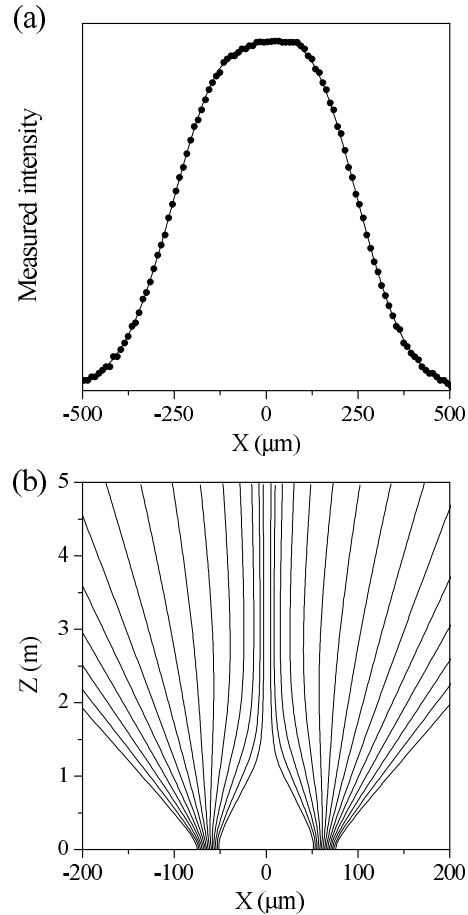


**Fig. 2.** a) Intensity obtained from reduced quantum trajectory (●) and standard quantum mechanics (solid line) calculations for a double-slit experiment with cold neutrons and  $\tau_c = 0$  (null coherence). b) Sample of reduced quantum trajectories illustrating the dynamics associated with the results shown in part (a).

agreement with the corresponding standard quantum mechanical calculations. This agreement indicates the suitability of equation (26) to describe the decoherence process here. In Figure 1(b) a sample of trajectories illustrating the dynamics associated with the results of Figure 1(a) is displayed. Here we see that as the outgoing neutron beams start to interfere (at a distance of  $\sim 1$  m from the two slits), some trajectories, mainly those closest to the symmetry axis of the experiment, start to show a conspicuous change of direction which is typical in the Bohmian description of interference processes [34, 35, 36]. However, due to the interference quenching, the extent of this behavior is reduced in both space and time: in space because the interference effects are stronger for the innermost trajectories [which give rise to the central peaks in Figure 1(a)] and in time because the time-of-flight of the neutrons,  $t_f$ , is such that  $t_f > \tau_c$ .

In Figure 2 we show the results for the extreme case of maximal decoherence, that takes place for  $\tau_c = 0$ . Similarly to what we did in Figure 1, the statistical results obtained by means of quantum trajectories and standard

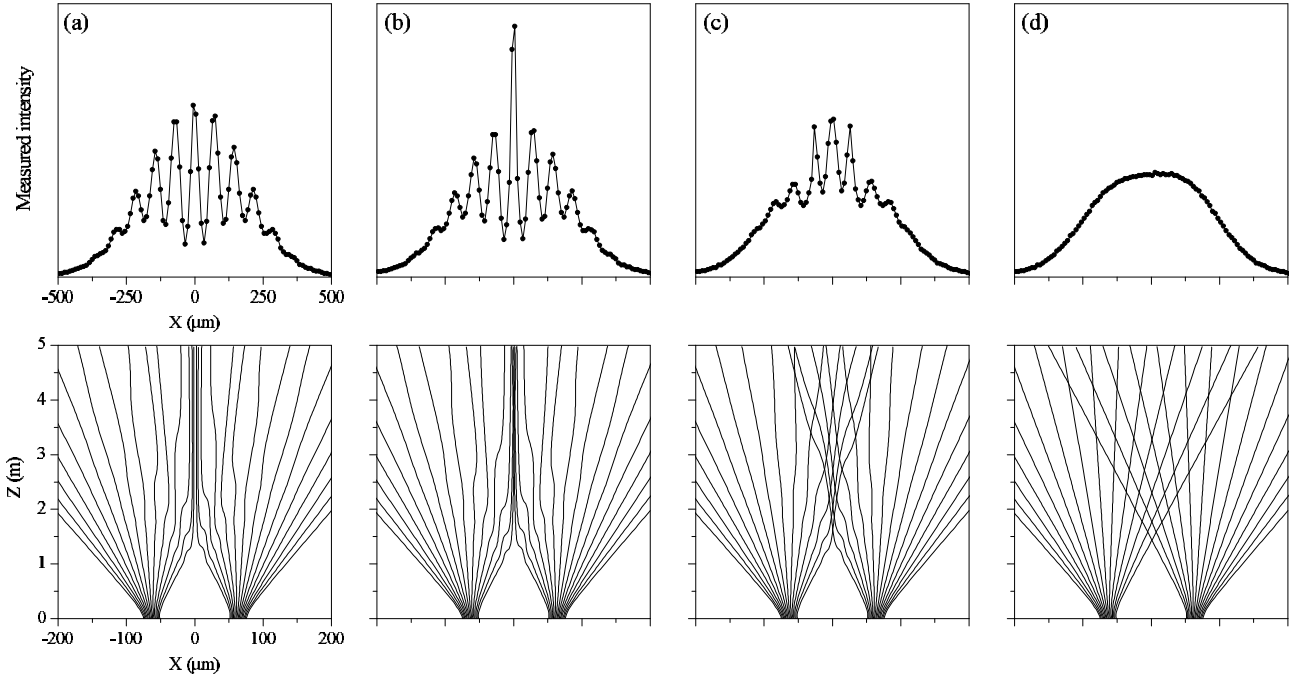


**Fig. 3.** Top: Intensity obtained after counting of the corresponding pseudo-reduced quantum trajectories for: a)  $\eta = \infty$ , b)  $\eta = 10$ , c)  $\eta = 1$ , and d)  $\eta = 0.1$ . The results from the counting (full circles) have been joined by means of B-splines (solid line) in order to facilitate their understanding. Bottom: Samples of trajectories illustrating the dynamics of the results shown in the upper part.

quantum mechanics (a), as well as a sample of representative trajectories (b) are plotted. Notice that despite the fact that there is no coherence here, trajectories do not cross the symmetry axis separating the regions covered by each slit. This is a manifestation of the contextual character of quantum trajectories. On the other hand, the absence of interference prevents the particles from undergoing the typical “wiggling” motion leading to the different diffraction channels [36], although still being non-locally correlated with other particles.

Therefore, we can conclude that within this first trajectory model, decoherence, simply understood as interference quenching, is not enough to suppress (or screen) the information concerning the initial context, and then to lead to a pure classical-like quantum dynamics (context-independent).

## 4.2 Screening of empty-slit information

In order to illustrate how the additional mechanism leading to the screening of the information provided by the empty slit works, we show in Figure 3 results obtained from equation (26), where  $c_1$  and  $c_2$  have been substituted by  $c'_1$  and  $c'_2$ , respectively. In this figure, results for different values of the parameter  $\eta$  (in increasing order from left to right) have been represented. As before, the statistics of quantum trajectories are given in the top row, and samples of quantum trajectories illustrating the corresponding dynamics in the bottom one. Notice that, as mentioned in Section 2, depending on the value of  $\eta$  two

dynamics can be clearly distinguished. For smaller values of  $\eta$  [see Figure 3(a)], a very slow decoupling is observed. Thus, the non-crossing effect dominates the system dynamics. On the other hand, for much higher values of  $\eta$ , the information about the empty slit is lost faster than the interference damping takes place, and some trajectories can cross the symmetry axis of the experiment. For total decoupling, trajectories display classical-like behavior. This fast screening is similar to that produced by a detector installed with the purpose of observing which slit the particle passed through.

The transition from one regime to the other one is also interesting both from the dynamical and the statistical points of view. As  $\eta$  increases an order of magnitude, a set of trajectories densely concentrates along the symmetry axis, a region where before there was a strong quantum force preventing the approach of trajectories. Thus, the central intensity maximum is remarkably enhanced, as can be seen in Figure 3(b), when compared with the same peak in Figure 3(a). This enhancement occurs at the expense of the intensity of the other maxima. That is, there is a transfer of trajectories from the outermost to the innermost diffraction channels. Dynamically, once the strong boundary imposed by the quantum potential along the symmetry axis (which is stronger than along the directions separating the different diffraction channels [36]) is suppressed, the “quantum pressure” [36,37] pushes the trajectories towards the region covered by the empty slit, and favors their transfer from one diffraction channel to the nearby one.

As  $\eta$  is further increased, quantum trajectories are also able to penetrate more across the symmetry axis, as it is apparent in Figure 3(c). The availability of a wider accessible region in the other side of the symmetry axis makes the concentration of trajectories along this direction to decrease, and they distribute more homogeneously. This causes a remarkable decrease of the coherence degree in the measured intensity, although the central peaks are still relatively intense. This trend continues until the interference pattern completely disappears when the decoupling is maximum [see Figure 3(d)]. In this case, the trajectories are unaffected by the presence of the other slit, i.e., they display a totally classical-like behavior. Moreover, a full transition from a dynamics characterized by single-valuedness of the momentum to another where it is bi-valued is observed, taking place this process within the system subspace.

## 5 Conclusions

Trajectory-based approaches have received much attention in the last years as a potential tool to handle and study high-dimensional complex quantum phenomena [26]. Nowadays the design of new numerical tools basically relies on this kind of formalisms rather than using other approaches based on the time-dependent Schrödinger equation. In the particular case of Bohmian mechanics, apart from the considerable interest that this theory has attracted, since providing a causal interpretation of quantum mechanics, it also possesses an intrinsic heuristic value which arises from its computational potential and physical insight, which are unavailable in standard quantum mechanics. The simple trajectory models considered here can be treated at the same level than Bohmian mechanics, providing a clear, intuitive and understandable picture of decoherence processes, which makes this concept more accessible.

The interference quenching is apparent in the double-slit experiment, where the elimination of interference fringes gives rise to a classical-like pattern where the classical addition rule of probabilities holds. In order to elucidate and understand how decoherence causes this interference quenching, we have considered here the simple trajectory based models mentioned above. As is well-known, in this experiment, the interference arises from the possibility for a particle to follow two different paths, from each slit to the detector. Within our trajectory description, we show that decoherence does not ensure that the particle motion related to one of those pathways is unaffected by the other one. Quantum mechanically decoherence suppresses the interference produced by the coherent superposition of the partial waves corresponding to each pathway. This gives rise to a classical-like intensity pattern, i.e., identical to that directly obtained from the sum of the intensities associated with those partial waves. However, the topology of the reduced quantum trajectories reveals that the particle motion is strongly influenced by both pathways even in the case of full decoherence. Thus, it is clear that a realistic decoherence model should reproduce both effects, the interference damping and the decoupling from the information

provided by the empty slit. The results shown here indicate that, although statistics erases the information about the interference, there is still a strong influence with a contextual nature in the behavior of the system. Note, on the other hand, that these simplistic models have allowed to avoid a realistic simulation, which constitutes a hard computational task. By using a simple model, here we have illustrated how the process leading to the loss of information coded by the empty slit not only causes such an effect, but provides an insight on a possible smooth transition from a quantum to a classical dynamics (i.e., how quantum trajectories become classical smoothly). Along this transition, the contextual dependence and non-local correlations are gradually suppressed. This mechanism allows one to understand decoherence from a broader perspective than that in which we have only suppression of interference. Also it can guide the design to new experiments in the mesoscopic regime (may be with larger particles than fullerenes, and/or a controllable environment), where the rules of quantum mechanics “dilute”, and objects can be described by means of classical dynamics. The fact that under certain conditions the central maximum of the intensity pattern gets relatively intense in comparison with the rest of maxima [like in Figure 3(b)] would reveal such a transition. Moreover, it is also important to stress that the structure of the quantum trajectories used here allows one to distinguish between one experiment performed with each slit independently open and another one with total decoherence and both slits simultaneously open.

## Acknowledgements

This work has been supported by the Ministerio de Educación y Ciencia (Spain) under projects MTM2006-15533, CONSOLIDER 2006-32, and FIS2007-62006; Comunidad de Madrid under the project S-0505/ESP-0158; and Agencia Española de Cooperación Internacional under the project A/6072/06. ASS would also like to thank the Ministerio de Educación y Ciencia for a “Juan de la Cierva” Contract.

## References

1. W.H. Zurek, *Physics Today* **44**(10), 36 (1991).
2. D. Giulini, E. Joos, C. Kiefer, J. Kupsch, I.-O. Stamatescu, and H.D. Zeh, *Decoherence and the Appearance of a Classical World in Quantum Theory* (Springer, Berlin, 1996).
3. R. Omnès, *Rev. Mod. Phys.* **64**, 339 (1992).
4. C. Kiefer and E. Joos, *Decoherence: Concepts and Examples*, in *Quantum Future*, Eds. P. Blanchard and A. Jadczyk (Springer, Berlin, 1998).
5. We would like to distinguish here between classical limit and decoherence as means to reach classical-like behaviors in quantum systems. In the first case we usually deal with *isolated* systems which, by varying a certain parameter, can display behaviors that resemble classical ones in average [see, for instance, A.S. Sanz, F. Borondo, and S. Miret-Artés *Europhys. Lett.* **55**, 303 (2002)]. On the other hand, in the second case, the averaging over the environment degrees of freedom causes that the quantum system

- exhibits a classical behavior. This is therefore not produced by varying a parameter, but by entanglement with the environment.
6. The environment may consist of collision events occurring during the system time-evolution or just the own internal degrees of freedom of the system (rotations, vibrations, etc.).
  7. M.A. Nielsen and I.L. Chuang, *Quantum Computation and Quantum Information* (Cambridge University Press, Cambridge, 2000).
  8. R.P. Feynman, R.B. Leighton, and M. Sands, *The Feynman Lectures on Physics* (Addison-Wesley, Reading, MA, 1965) Vol. 3.
  9. C.J. Davisson and L.H. Germer, Phys. Rev. **30** 705 (1927).
  10. B. Brezger, L. Hackermüller, S. Uttenthaler, J. Petschinka, M. Arndt, and A. Zeilinger, Phys. Rev. Lett. **88** 100404 (2002).
  11. A. Tonomura, J. Endo, T. Matsuda, T. Kawasaki, and H. Ezawa, Am. J. Phys. **57**, 117 (1989).
  12. F. Shimizu, K. Shimizu, and H. Takuma, Phys. Rev. A **46**, R17 (1992).
  13. L.I. Schiff, *Quantum Mechanics* (McGraw-Hill, Singapore, 1968) 3rd Ed.
  14. R. Mir, J.S. Lundeen, M.W. Mitchell, A.M. Steinberg, J.L. Garretson, and H.M. Wiseman, New J. Phys. **9**, 287 (2007).
  15. W.K. Wootters and W.H. Zurek, Phys. Rev. D **19**, 473 (1979); R. Bhandari, Phys. Rev. Lett. **69**, 3720 (1992); B.-G. Englert, Phys. Rev. Lett. **77**, 2154 (1996); H.M. Wiseman, F.E. Harrison, M.J. Collet, S.M. Tan, D.F. Walls, and R.B. Killip, Phys. Rev. A **56**, 55 (1997); G. Björk and A. Karlsson, Phys. Rev. A **58**, 3477 (1998); S. Dürr, Phys. Rev. A **64**, 042113 (2001).
  16. S. Dürr, T. Nonn, and G. Rempe, Phys. Rev. Lett. **81**, 5705 (1998).
  17. E. Joos and H.D. Zeh, Zeit. Phys. **59B**, 223 (1985).
  18. D. Bohm, Phys. Rev. **85**, 166, 180 (1952).
  19. P.R. Holland, *The Quantum Theory of Motion* (Cambridge University Press, Cambridge, 1993).
  20. R.E. Wyatt, *Quantum Dynamics with Trajectories: Introduction to Quantum Hydrodynamics* (Springer, Berlin, 2005).
  21. A.S. Sanz and F. Borondo, Eur. Phys. J. D **44**, 319 (2007).
  22. A. Zeilinger, R. Gähler, C.G. Shull, W. Treimer, and W. Mampe, Rev. Mod. Phys. **60**, 1067 (1988).
  23. H.-P. Breuer and F. Petruccione, *The Theory of Open Quantum Systems* (Oxford University Press, Oxford, 2002).
  24. P. Pechukas and U. Weiss (Eds.), *Quantum Dynamics of Open Systems*, special issue in Chem. Phys. **268** (2001).
  25. I. Percival, *Quantum State Diffusion* (Cambridge University Press, Cambridge, 1998).
  26. D. Micha and I. Burghardt (eds.) *Quantum Dynamics of Complex Molecular Systems* (Springer, Berlin, 2006).
  27. W.H. Miller, J. Chem. Phys. **53**, 3578 (1970); W.H. Miller, Faraday Discuss. **110**, 1 (1998); R. Gelabert, X. Giménez, M. Thoss, H. Wang, and W.H. Miller, J. Phys. Chem. A **104**, 10321 (2000); R. Gelabert, X. Giménez, M. Thoss, H. Wang, and W.H. Miller, J. Chem. Phys. **114**, 2562 (2001); R. Gelabert, X. Giménez, M. Thoss, H. Wang, and W.H. Miller, J. Chem. Phys. **114**, 2572 (2001); S. Zhang and E. Pollak, J. Chem. Phys. **121**, 3384 (2004).
  28. S.M. Tan and D.F. Walls, Phys. Rev. A **47**, 4663 (1993).
  29. C.M. Savage and D.F. Walls, Phys. Rev. A **32**, 2316, 3487 (1985).
  30. T. Qureshi and A. Venugopalan, Int. J. Mod. Phys. (to appear, 2007); *Preprint* quant-ph/0602052.
  31. A.S. Sanz, F. Borondo, and M. Bastiaans, Phys. Rev. A **71**, 42103 (2005); A.S. Sanz and F. Borondo, Phys. Rev. A (accepted, 2008).
  32. Throughout this work, we indicate time-dependence by a subscript “ $t$ ” [ $A_t \equiv A(t)$ ], while initial values do not carry any label [ $A \equiv A(0)$ ].
  33. M. Born, Z. Physik **37**, 863 (1926); Nature **119**, 354 (1927).
  34. C. Philippidis, C. Dewdney, and B.J. Hiley, Nuovo Cimento B **52**, 15 (1979); C. Philippidis, D. Bohm, and R.D. Kaye, Nuovo Cimento B **71**, 75 (1982).
  35. A.S. Sanz, F. Borondo, and S. Miret-Artés, Phys. Rev. B **61**, 7743 (2000).
  36. A.S. Sanz, F. Borondo, and S. Miret-Artés, J. Phys.: Condens. Matter **14**, 6109 (2002).
  37. R. Guantes, A.S. Sanz, J. Margalef-Roig, and Miret-Artés Surf. Sci. Rep. **53**, 199 (2004).